Dynamical Systems Theory Sheds New Light on Compound Climate Extremes in Europe and Eastern North America

De Luca, P.[a,b,c,*], Messori, G.[b,d], Faranda, D.[e,f]

[a] *Geography and Environment, Loughborough University, Loughborough, UK*
[b] *Department of Earth Sciences, Uppsala University, Uppsala, Sweden*
[c] *Centre of Natural Hazards and Disaster Science (CNDS), Uppsala, Sweden*
[d] *Department of Meteorology, Stockholm University and Bolin Centre for Climate Research, Stockholm, Sweden*
[e] *Laboratoire des Sciences du Climat et de l'Environnement, LSCE/IPSL, CEA-CNRS-UVSQ, Université Paris-Saclay, Gif-sur-Yvette, France*
[f] *London Mathematical Laboratory, London, UK*

Abstract

The interactions between different meteorological hazards can result in socio-economic damages exceeding those expected from the individual hazard components. Such combinations of hazards are commonly known as multi-hazards or compound extremes. Here, we propose a novel approach to the study of compound extremes grounded in dynamical systems theory. Specifically, we present the co-recurrence ratio (α), which elucidates the dependence structure between fields by quantifying their joint recurrences. This approach is applied to daily climate extremes, derived from the ERA-Interim reanalysis over the 1979-2018 period. The analysis focuses on concurrent (i.e. *same-day*) wet (total precipitation) and windy (10m wind gusts) extremes in Europe and concurrent cold (2m temperature) extremes in Eastern North America and wet extremes in Europe. Results for Europe show that α peaks during boreal winter. Climate anomalies observed during α extremes resemble those associated with the positive North Atlantic Oscillation. These are situations which correspond to extra-tropical cyclones impacting North-Western Europe, resulting in frequent wet and windy extremes. For the East-

*Corresponding author
Email address: p.deluca@lboro.ac.uk (De Luca, P.)

ern North America-Europe case, α extremes once again reflect the concurrent climate extremes, and correspond to cold extremes over North America and wet extremes over Europe. The co-recurrence ratio (α) therefore reflects the evolution of the chosen meteorological fields, and successfully characterises compound extremes. This approach is entirely general, and may be applied to different types of compound extremes and geographical regions.

Keywords: Dynamical Extremes, Dynamical Systems Theory, Compound Extremes, Multi-Hazards, Climate Dynamics, Climate Extremes

1. Introduction

Individual natural hazards can interact [1], often resulting in high-impact events leading to heavy socio-economic losses [2, 3, 4]. These events are known as multi-hazards and they are explicitly defined by The United Nations Office for Disaster Risk Reduction (UNDRR) as *(1) the selection of multiple major hazards that the country faces, and (2) the specific contexts where hazardous events may occur simultaneously, cascadingly or cumulatively over time, and taking into account the potential interrelated effects* [5]. Multi-hazards are also known as compound events or compound extremes [2, 4].

In recent years the concept of compound extremes, also extended to include multi-risks, has attracted the attention of the scientific community [e.g. 6, 7, 8, 9, 10, 11, 12, 13]. These extremes have potentially major implications for a wide range of private and public stakeholders including policy makers, (re)insurance companies, governments and local communities around the world [e.g. 14, 15]. Identifying compound extremes and quantifying their observed [16, 17, 18, 19] and future projected [3, 20] spatio-temporal characteristics is thus a highly scientifically and socio-economically relevant goal, which supports disaster risk reduction through increased understanding of risks and enhancement of resilience [2, 5, 11].

Statistical models are required to adequately assess the risk of compound (or concurrent) extremes and to evaluate numerical models. However, compound extremes are inherently complex: they are rare, multivariate, and live in a sparsely sampled region of a multidimensional space with limited observational coverage. Statistical models thus rely heavily on extrapolation. A wide range of techniques have been proposed to study compound

extremes, ranging from multivariate extreme value statistical models based on copula assumptions [e.g. 21, 22, 23, 24], to max-stable models [e.g. 25, 26], conditional exceedance models [e.g. 27, 28, 29, 30, 31], Bayesian models [32, 33, 34, 35] and the multivariate skew-t distribution [36, 37]. All these approaches can provide only limited information about the chaotic and spatial behaviour of atmospheric variables. Indeed, incorporating the latter requires complex extensions of these methods [38, 39], often with a risk of overfitting the statistical model.

Here, we propose a novel approach grounded in dynamical systems theory which overcomes some of these limitations, and aims to provide a complementary view to more traditional analyses issuing from statistics and climate dynamics [e.g. 40, 41]. We specifically propose an objective measure of the co-recurrence of extremes in different climate variables, which can provide both temporal and spatial information and can be linked to the underlying dynamical properties of the climate system, as well as explicitly accounting for its underlying chaotic nature. This is complemented by two other indicators characterising the evolution of large-scale climate fields [42, 43, 44]. The approach is very flexible, and can in principle be applied to any number of variables, geographical region and type of dataset. Within the text, we adapt the vocabulary used in the literature to fit the novel approach we propose. We will be referring to *compound* extremes when considering multivariate metrics calculated from dynamical systems theory and to *concurrent* extremes when discussing the joint occurrences (i.e. *same-day*) of extreme values in the climate variables.

We begin by providing a brief description of our methodology (Section 2). Next, we illustrate the physical interpretation of the different dynamical systems metrics and their seasonality (Section 3.1.1), and present an application to concurrent wet and windy extremes in Europe (Section 3.1.2), along with concurrent cold extremes in Eastern North America and wet extremes in Europe (Section 3.2). We thus address concurrent extremes at both single and separate geographical regions. Our choice is motivated by the significant scientific and media attention that both wet and windy weather in Europe [e.g. 45, 46, 47, 48] and cold spells in North America [e.g. 49, 50, 51] has attracted in recent years. The analysis in Section 3.1 primarily aims to relate the information provided by our metrics to known features of the atmospheric variability over the Euro-Atlantic region, and can be viewed as a test of the

robustness of the indicators we propose. Section 3.2 instead illustrates how our approach can be used to gain novel insights into concurrent extremes in two different regions. We conclude by discussing our results in the context of the literature on these classes of extremes (Section 4).

2. Data and Methods

2.1. Data

We use ECMWF's ERA-Interim reanalysis [52], at a horizontal resolution of 0.75°, from 1979 to 2018. The analysis was conducted on daily data at 12 and 00 UTC (12h step) of total precipitation (mm) and 10m wind gust (m/s). To obtain a unique daily value, these were then summed and averaged, respectively. We also used 2m temperature at 00, 06, 12 and 18 UTC, which were averaged as daily observations. From now on we will refer to these variables simply as precipitation, wind and temperature. We consider two domains: Europe (18°W–51°E, 30°N–75°N) and Eastern North America (99°W–75°W, 30°N–51°N). Daily data over 1979-2018 for the North Atlantic Oscillation (NAO) [53], the dominant mode of climate variability within the North Atlantic region, were downloaded from the NOAA - Climate Prediction Center website (available here).

2.2. Dynamical systems metrics

We use three dynamical systems metrics: the local dimension (d); the local persistence (θ^{-1}); and the local co-recurrence ratio (α) [42, 54]. d and θ^{-1} are calculated for both univariate and multivariate cases, whereas α always refers to two different variables. All three metrics are local in phase-space, and instantaneous in time. Their calculation issues from the application of extreme value theory to Poincaré recurrences [44]. In this approach, the atmospheric dynamics is considered as chaotic but settled on an attractor – namely the set of states that the system approaches repeatedly. The three metrics can then be computed for any state ζ on the attractor – in our case a latitude-longitude field of one or more variables at a given time. d and θ^{-1} have recently been applied to a range of different climate fields over different geographical domains and were found to successfully reflect large-scale features of atmospheric motions [55, 42, 56, 54, 43, 57, 58].

The local dimension $d(\zeta)$ describes the evolution of the system around (ζ), and can be interpreted as a proxy for the number of degrees of freedom

active around the state of interest. The local persistence $\theta^{-1}(\zeta)$ measures the mean residence time of the system around such state. A high (low) persistence indicates that the systems evolution will slowly (rapidly) lead to a dynamically different state. The higher the value of θ^{-1}, the more likely it is that the preceding and future states will resemble ζ over comparatively long timescales [42, 43, 57]. The two dynamical systems indicators can be computed for both individual climate fields (e.g. sea-level pressure 42) and multiple fields jointly [54]. The derivation of d and θ^{-1} is based on defining recurrences in terms of a given distance metric *dist* between all states visited by the system. For details we refer the reader to the Supporting Information here, Appendix A of [59] and [60].

The multivariate d and θ^{-1} metrics are derived following [54]. Given two variables $x(t)$ and $y(t)$, we can define a state on the Poincaré section jointly spanned by x and y as $\zeta = \{\zeta_x, \zeta_y\}$. Joint logarithmic returns of this state are then given by:

$$g(x(t), y(t)) = -\log \left[\text{dist} \left(\frac{x(t)}{\|x\|}, \frac{\zeta_x}{\|x\|} \right)^2 + \text{dist} \left(\frac{y(t)}{\|y\|}, \frac{\zeta_y}{\|y\|} \right)^2 \right]^{\frac{1}{2}} \quad (1)$$

Where the negative logarithm is applied to increase the discrimination of close recurrences and $\|.\|$ represents the average root mean square norm of vector's coordinates and *dist* is the Euclidean Norm. We can further define $d_x(\zeta)$ and $d_y(\zeta)$, the dimensions of the Poincaré sections defined by x and y around ζ, with respect to the chosen distance metric. From Eq. (1) one can obtain the *co-dimension* $d_{x,y}$ analogously to the derivation of the univariate d (for ease of notation we hereafter drop the dependence on ζ). The co-dimension has the following property:

$$\min(d_x, d_y) \leq d_{x,y} \leq d_x + d_y \quad (2)$$

The case $d_{x,y} = d_x + d_y$ implies no coupling bewteen x and y. If instead the variables are deterministically coupled (i.e. x is a function of y or viceversa), $d_{x,y} = \min(d_x, d_y)$.

Following the definition of joint logarithmic returns given in Eq. (1) and as for d above, one can also define the local *co-persistence* $\theta_{x,y}^{-1}$. This is

defined as a weighted average of θ_x^{-1} and θ_y^{-1}, where the weights depend on the size of the hyper-ball around ζ in the Poincaré sections x and y [54, 61].

Along with $d_{x,y}$ and ${\theta_{x,y}}^{-1}$ we adopt a phase-space local measure of dependence first introduced in [54]. The co-recurrence ratio $0 \leq \alpha(\zeta) \leq 1$ of a state $\zeta = \{\zeta_x, \zeta_y\}$ is defined as:

$$\alpha(\zeta) = \frac{\Pr[g(x(t)) > s_x(q) | g(y(t)) > s_y(q))]}{\Pr[g(x(t)) > s_x(q)]} \tag{3}$$

Where $s_x(q)$ and $s_y(q)$ are high q-th quantiles (or thresholds) of the univariate logarithmic returns $g(x(t))$ and $g(y(t))$. When $\alpha(\zeta) = 0$ no co-recurrences of $\zeta = \{\zeta_x, \zeta_y\}$ are observed in the phase-space, when we observe a recurrence of ζ_x. Intuitively, when $\alpha(\zeta) = 1$, all the co-recurrences of $\zeta = \{\zeta_x, \zeta_y\}$ also correspond to recurrences of ζ_x, and viceversa. In other words, α quantifies the probability of co-recurrences of two (or more) variables within an hyper-ball around ζ. For more detailed information about the multivariate dynamical systems metrics we refer the reader to [54].

2.3. Statistical Analysis

2.3.1. Definition of anomalies and extremes

We define anomalies relative to a daily mean climatology. For example, the climatological temperature at a given gridpoint for the 19^{th} February is the mean of all 19^{th} February temperatures at that location over the 40 years considered here. Precipitation and wind extremes are defined as daily values $> 99^{th}$ quantile, whereas cold temperature extremes are daily observations $< 1^{st}$ quantile of the respective distributions at each gridpoint. The selection was performed on absolute values, rather than anomalies, in the spirit of an impacts-based perspective. Indeed, a very strong windstorm is more likely to cause damage than an out-of-season (and thus extreme in terms of anomalies) but moderate (in terms of absolute wind-speed values) windstorm, although out-of-season extremes are associated with their own specific sets of risks. The same analysis was also performed for extremes based on anomalies of the climate variables and the two approaches show a marked spatio-temporal agreement (see Supporting Information).

The anomalies of precipitation, wind and temperature are stratified according to α daily extremes ($> 99^{th}$ quantile), thus informing on the behaviour of the climate variables under strong dynamical coupling conditions.

We also consider, for each gridpoint, the composite α mean anomalies associated with univariate and concurrent extremes of precipitation, wind and temperature. This informs on the strength of the dynamical coupling observed during the different sets of climate extremes. A list of extreme occurrences at each gridpoint was compiled, and then the corresponding daily α anomalies were composited, thus providing a different composite α mean anomaly value at each gridpoint. For example, let us consider precipitation and wind extremes for a gridpoint within the European region. First, we identified days when the two extremes (co)occurred at that location, and then we computed the α mean anomalies based on those days (note that the α daily values are the same for both extremes, since it is computed using both variables simultaneously). For the case of concurrent cold and wet extremes in Eastern North America and Europe respectively, we adopted a similar procedure: i) identify dates on which at least one gridpoint in each domain displays an extreme observation; ii) identify all gridpoints displaying extreme values on each selected date; and iii) calculate the α mean anomalies for each selected gridpoint over the two regions. Note that, again, α daily values are the same for both variables, regardless of the fact that they are considered over different geographical domains. In the figures we only show α mean anomalies $> 90^{th}$ quantile of the full α distribution for each pair of variables, to highlight the spatial patterns of the most extreme observations.

2.3.2. Statistical testing

The significance of the anomalies in both the climate variables and α extremes is evaluated using a boot-strapping (n=1000 samples) analysis. The detailed procedure is provided in the Supporting Information.

The robustness of the α anomaly means observed during univariate and concurrent extremes was also assessed by performing a sign test. This quantifies the fraction of individual extreme observations at a given gridpoint which have the same sign anomaly as the overall composite. For example, a sign test value of 66% at a location with a positive α composite anomaly means that 66% of the days used to create the composite display a positive α daily anomaly, while 34% display a negative anomaly. Clearly, the higher the % of members sharing same-sign anomalies, the more robust the results are.

3. Results

3.1. Wet and windy extremes in Europe

3.1.1. Compound dynamical extremes

In Figure 1 we show both compound and univariate dynamical indicators of precipitation and wind in Europe. α peaks during boreal winter (Dec-Feb) with values of $\sim$0.15 and reaches its lowest values during spring ($\sim$0.075) and summer ($\sim$0.10, Figure 1a). The α winter peak follows the intuition that during these months the passage of extra-tropical cyclones (ETCs) over western-continental Europe and the British Isles (BI) can lead to widespread flooding episodes and comparatively frequent concurrent wet and windy extremes [16, 62, 63, 64]. On the other hand, the lower α values observed during spring and in particular summer reflect wet extremes which are mainly driven by small-scale convective processes [e.g. 65] and therefore have a weaker link to both the synoptic and larger-scale circulation and wind extremes [66].

Negative d anomalies during α extremes (i.e. strong dynamical coupling) are observed for both the compound and univariate cases (Figure 1b), with the former and precipitation being respectively the ones with more/less numerous negative anomalies. A similar, albeit less pronounced, pattern of negative values is found for θ^{-1} anomalies (Figure 1c), with precipitation still being the observable showing the weaker deviation from climatology. Low d and θ^{-1} are associated with predictable configurations [42, 43, 67], and we find here that this matches a strong coupling of the large-scale configurations of different variables.

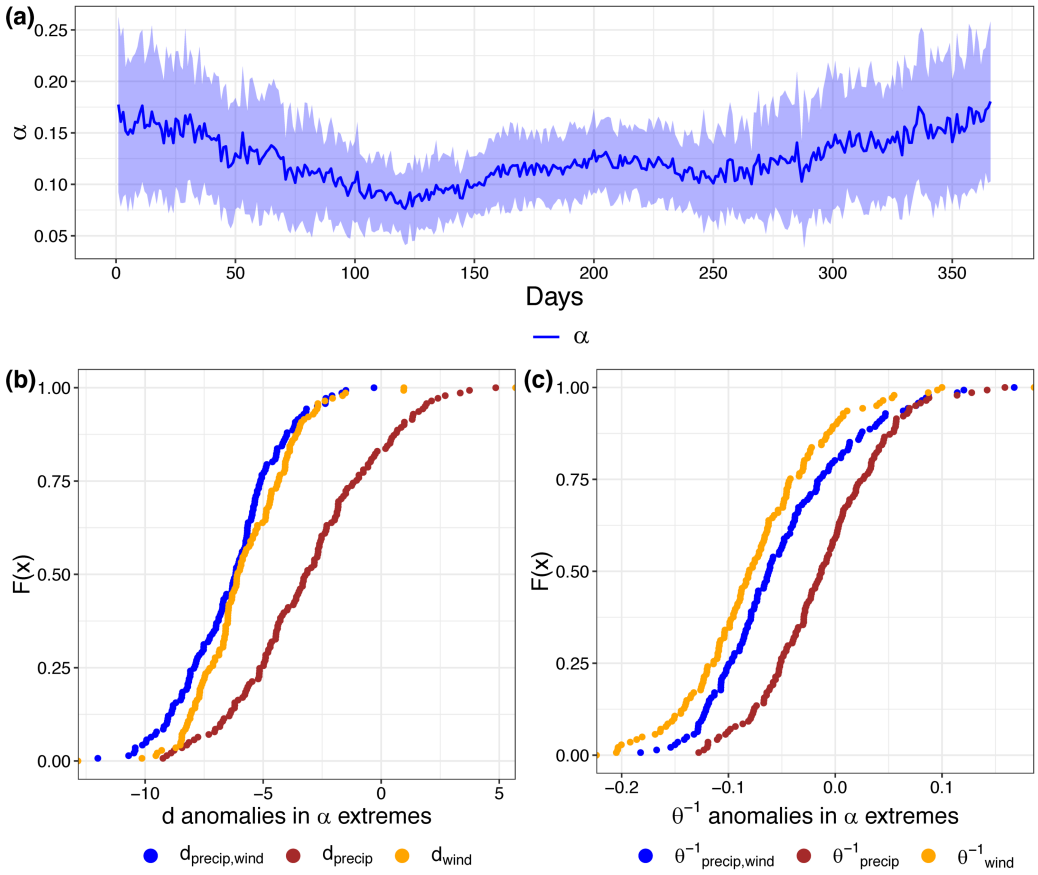

Figure 1: **(a)** Daily climatological means for the co-recurrence ratio (α) of total precipitation (mm) and 10m wind gust (m/s). **(b)** Cumulative distribution functions (CDFs) of local dimension (d) anomalies associated with α daily extremes ($> 99^{th}$ quantile); **(c)** as **(b)** but for local persistence (θ^{-1}). In **(b)-(c)** the metrics are calculated for total precipitation (brown), 10m wind gust (yellow) and jointly for the two (blue). Blue shaded areas in **(a)** represent one standard deviation from the daily climatological means. The data covers 1979-2018 over Europe (see text).

We next relate α to the NAO index (NAOI) [53]. The NAOI daily values during α extremes (Figure 2a) are overwhelmingly positive (mean=0.85, dashed line), and well above about what may be obtained by chance (dot-dashed line). When the NAO is in a positive phase, northern Europe experiences enhanced storminess from the passage of ETCs, which bring concurrent flooding and windstorms [16, 47, 68, 69]. This agrees with the strong negative anomalies in d and θ^{-1} discussed above, since the positive NAO has been previously identified as a low-d low-θ^{-1} configuration [42]. Moreover, the vast majority of α extremes occur during later autumn and winter, with no observations in May and summer (June-August, Figure 2b), further confirming the plausibility of a the link between α extremes and winter ETCs.

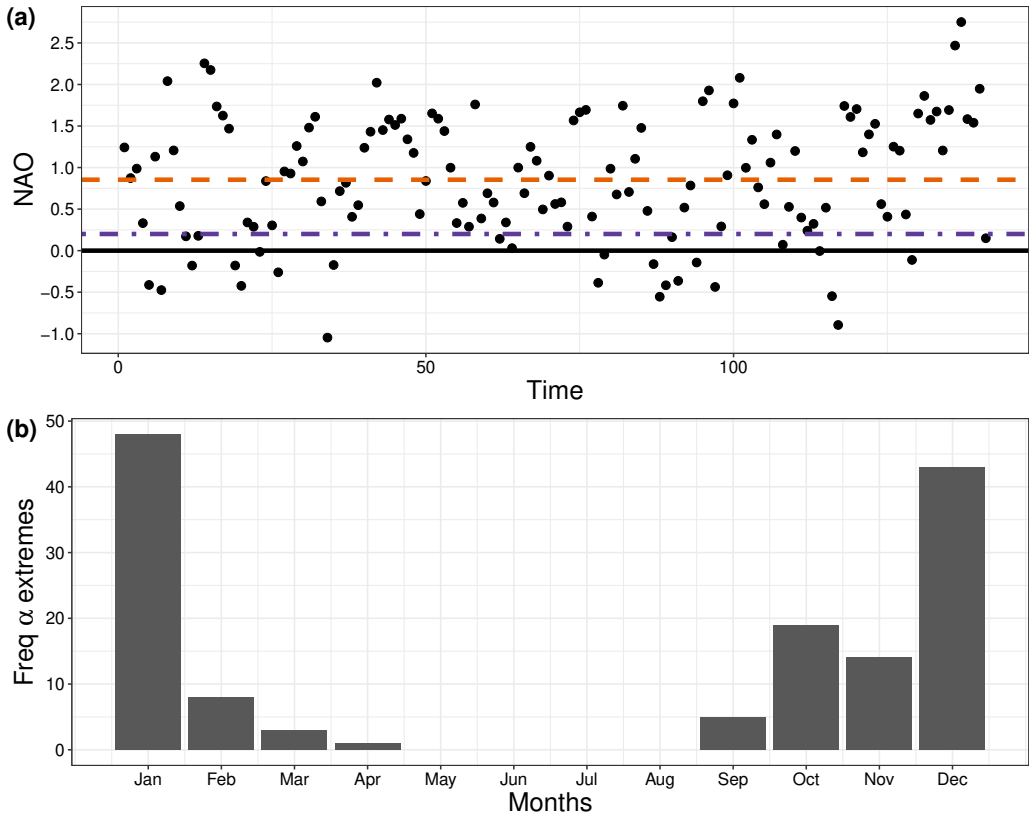

Figure 2: **(a)** Daily NAOI and **(b)** monthly frequencies for α daily extremes ($> 99^{th}$ quantile). In **(a)** the black solid line represents $NAOI = 0$, the orange dashed line the mean NAOI value for α extremes and the violet dot-dashed line the mean 97.5^{th} quantile NAOI obtained by random sampling (n=10000, no replacement) from the entire NAO daily time-series. The data covers 1979-2018.

3.1.2. Concurrent climate extremes

We next consider the link between α extremes and extremes in climate variables. During α extremes, positive anomalies in both the precipitation and wind gust fields are observed in northern Europe, over a broad region spanning the BI, the North Sea and the surrounding coastal areas. Negative anomalies are instead observed in southern Europe (Figure 3a-b). This pattern resembles that associated with the NAO (Figure S1), further strengthening our interpretation that α extremes are able to capture the impacts of ETCs in northern Europe.

The number of concurrent wet and windy extremes peaks during late boreal autumn and the winter months (Figure 3c). This closely reflects the timing of the α extremes (Figure 2b), proving additional evidence for a narrow link between compound dynamical and concurrent climate extremes.

Finally, we test the inverse link, namely whether large α values can be recovered when conditioning on extremes in the climate variables. The α anomaly means, conditioned on precipitation and wind extremes, are highest in north-western Europe (Figure 3d-e). Although the signal for precipitation is somewhat patchy, there is an overall good spatial correspondence with the regions displaying large anomalies in the climate variables themselves (Figure 3a-b). We also note that the α anomaly means related to wind extremes are higher than those for precipitation. This is not surprising, since the latter is a notoriously noisy and high-dimensional field [55]. α anomaly means calculated for concurrent wet and windy extremes mostly reflect the anomalies observed for the univariate extreme cases (Figure 3f). The largest values are again distributed over the BI, north-western and part of north-central Europe and the Nordic Seas. The α anomaly means for the concurrent extremes case show higher values than the ones for precipitation and wind alone. This is somewhat expected since the α metric is computed based on the dynamical coupling of the two observables. The sign test (stippling in Figure 3d-f) largely reflects this, and in general matches spatial patterns of the α anomaly means. The same analyses as shown in Figure 3c-f were repeated by using a different definition of extremes (see Section 2.3.1 and Figure S2). The results are consistent between the two approaches.

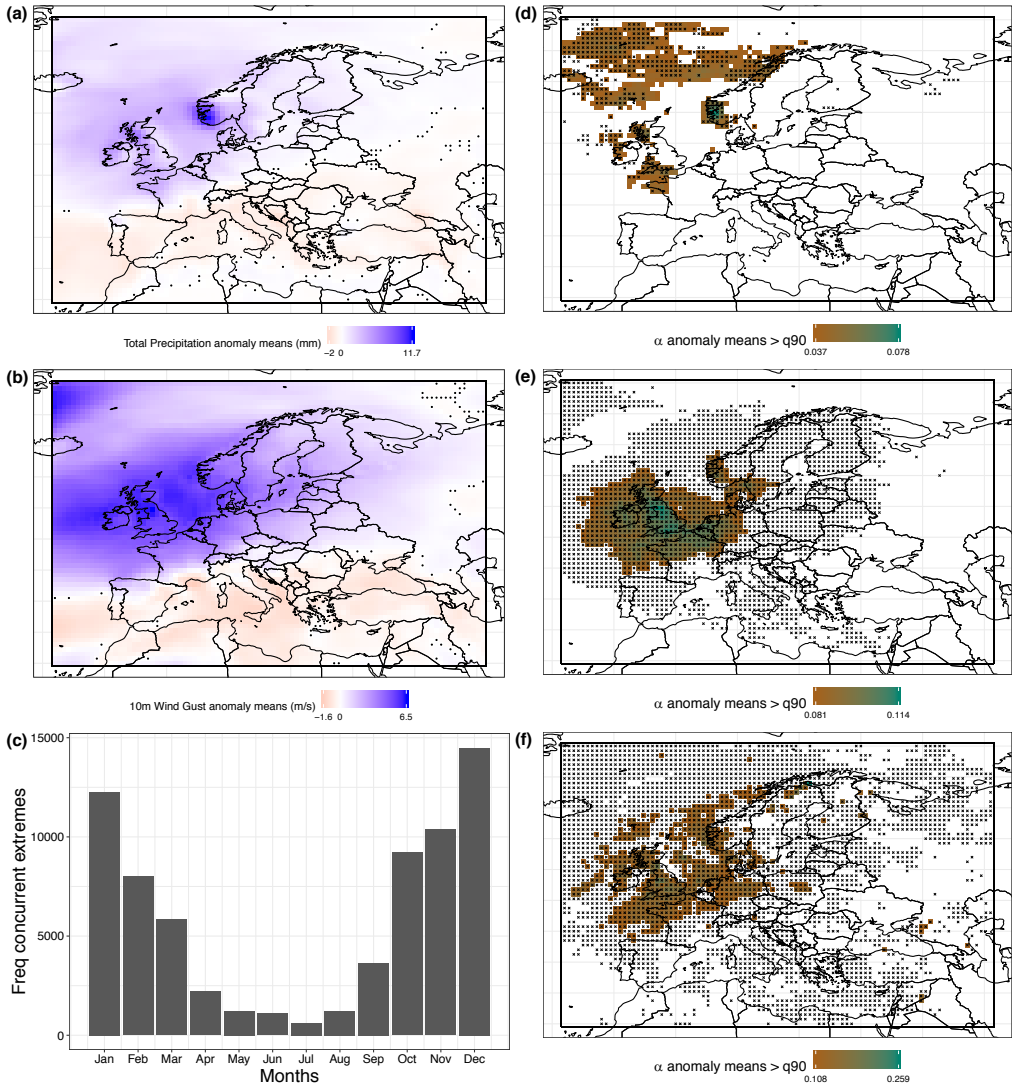

Figure 3: **(a)** Total precipitation (mm) and **(b)** 10m wind gust (m/s) anomaly means associated with α extremes ($> 99^{th}$ quantile). **(c)** Monthly frequencies of concurrent total precipitation and 10m wind gust extremes. α anomaly mean values ($> 90^{th}$ quantile), for each gridpoint, observed during **(d)** total precipitation, **(e)** 10m wind gust and **(f)** concurrent total precipitation and 10m wind gust extremes ($> 99^{th}$ quantile). In **(a)-(b)** stippling represents values not statistically significant (boot-strapping, n=1000 samples). In **(d)-(f)** only statistically significant values are plotted and stippling represents grid-points with >66% of daily α positive anomalies (sign test).

3.2. Cold and wet extremes in Eastern North America and Europe

In this section we consider a second set of concurrent extremes, namely temperature over Eastern North America and precipitation over Europe (Figure 4). α extremes are associated with negative temperature anomalies across Eastern North America, with the largest anomalies situated in the north-eastern part of the domain (Figure 4a). Precipitation anomalies in Europe are instead mostly positive, extending from Iberia to Western France and Scandinavia, as well as in the Eastern Mediterranean and Middle-East (Figure 4b). The vast majority of the concurrent cold and wet extremes are observed during boreal winter months (Dec-Feb). No co-occurrences are observed from April to October (Figure 4c).

Large α anomaly means ($> 90^{th}$ quantile) associated with cold extremes are observed over the north-eastern part of the North American domain (Figure 4d), reflecting the higher temperature anomaly patterns found in Figure 4a. α anomaly means linked with wet extremes in Europe again generally match the footprint of the precipitation anomalies (Figure 4e). Lastly, α anomaly means observed during concurrent cold and wet extremes are highest in the north-eastern North American domain and western European countries, from Portugal to central-southern Scandinavia (Figure 4f). These α anomaly means have higher values than for the univariate extreme cases, in a similar way as for concurrent wet and windy extremes in Europe (Figure 3f). This reflects α's strong link to the dynamical coupling of different fields and hence concurrent extremes. The sign test results are in agreement with the spatial distribution of the α anomaly means (Figure 4d-f). As for Figure 3c-f, similar results are retrieved for a different definition of extremes (Figure S3).

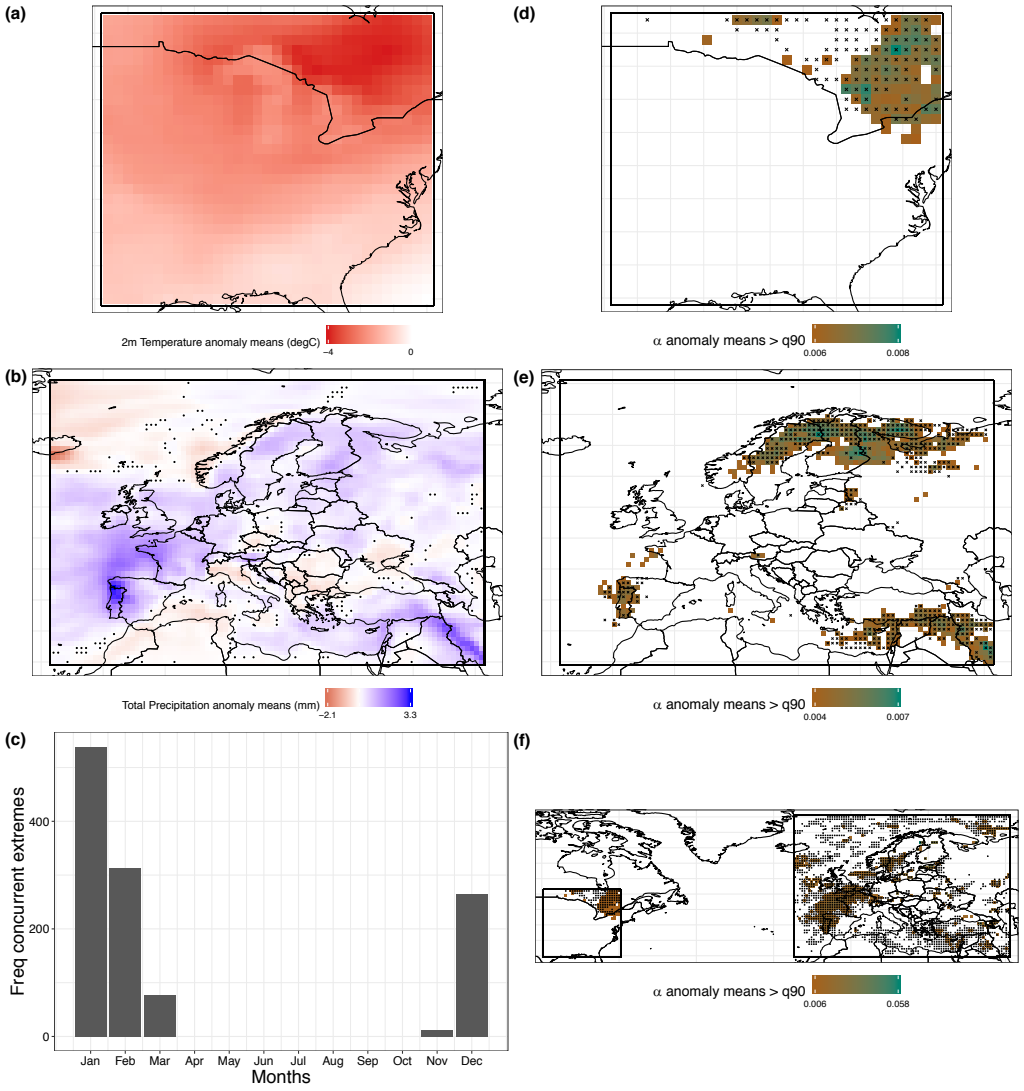

Figure 4: As Figure 3 but for 2m temperature ($^{\circ}C$) in Eastern North America and total precipitation (mm) in Europe. In **(d)** and **(f)** 2m temperature observations are daily values ($< 1^{st}$ quantile). In **(d)-(f)** only statistically significant values are plotted and stippling represents gridpoints with >60% of daily α positive anomalies (sign test).

4. Discussion and Conclusions

In this study we applied a new approach issued from dynamical systems theory [42, 44, 54] to the study of compound and concurrent climate extremes. We specifically focussed on wet and windy extremes in Europe and cold and wet extremes respectively in Eastern North America and Europe. We defined a coupling parameter α (the co-recurrence ratio) that measures the probability of joint recurrences of specific configurations in two climate variables. Almost by definition, α is sensitive to the chosen geographical domain(s). Indeed, the dynamical coupling between the variables of interest can change significantly when including or excluding data. It is therefore important to limit the analysis only to regions of interests, whatever the criterion for "interesting" may be. Two more dynamical systems metrics were also computed for both uni- and multivariate and compound cases, namely the local dimension (d) and the local persistence (θ^{-1}). These inform on the number of degrees of freedom active around a given state of the system (here the atmosphere in the Euro-Atlantic and Eastern North American sectors) and on the mean residence time of the system around such state, respectively.

The same approach could in the future be applied to a suite of renalysis products, to evaluating large ensembles of historical Atmosphere-Ocean General Circulation Models runs [e.g. 70, 71], or to projecting future changes in compound extremes under a warming climate. Moreover, the dynamical systems approach used here can be applied to any geographical region and set of climate variables (as long as the latter show a chaotic behaviour). A diverse set of compound and concurrent events can therefore be tested, and global hot-spots of compound extremes identified. There is also the hope that this methodology may help investigate outstanding questions; for example the role of Arctic Amplification in driving northern hemisphere mid-latitude weather and climate extremes [e.g. 72, 73, 74, 75].

The main findings of the study can be summarised as follows:

- The co-recurrence ratio α captures the seasonal cycle in extreme event occurrences for the domains (Eastern North America, Europe) and variables (precipitation, 10m wind gusts, 2m temperature) considered here.
- Highly coupled (high α) states correspond to more predictable configurations of the atmosphere (low d and θ^{-1} values) [42, 43, 67].

- α extremes, here termed compound extremes, match *same-day* extremes in the climate variables, here termed concurrent extremes. High α values indicate a strong coupling between the different climate variables, which intuitively should be the case for spatially and/or temporally co-occurring extremes.

- For the European domain, the close correspondence between extremes in α and the climate variables is mediated by the strong projection of α extremes on the positive phase of the NAO.

These findings highlight the ability of dynamical systems approaches to capture the spatio-temporal variability of the atmosphere. In Europe, our results mostly confirm the well-known link between a positive NAO and stormy weather over the North-Western part of the continent, leading to widespread flooding linked with severe winds [16, 47, 62, 63, 64]. The physical relationship between cold temperatures in Eastern North America and wet extremes in Europe is not as obvious. The notably wet and stormy winter of 2013/2014 in parts of Europe and the British Isles [e.g. 46, 47, 48] co-occurred with a very cold winter in the Eastern United States [49, 50]. Moreover, a recent study [51] explicitly addressed the question of possible physical links between winter cold spells in North America and wet and stormy events over western Europe. The authors concluded that cold spells in North America are a significant and plausible, but not necessary, precursor of stormy conditions in western Europe.

Our findings bring new insights into multi-hazards (or compound events) research. Our dynamical systems perspective is flexible, links directly to concepts of predictability and coupling and may be useful in both practical (e.g. numerical forecasting of extremes) and more theoretical (e.g. understanding the atmospheric drivers of extremes) contexts.

Author contribution

PDL performed the analyses, created the figures and wrote the first manuscript draft. GM and PDL conceived and designed the study. GM and DF provided the MATLAB code to compute the dynamical systems indicators. All the authors contributed to preparing the manuscript.

Acknowledgements

PDL was funded by a Natural Environment Research Council studentship awarded through the Central England NERC Training Alliance (CENTA http://www.centa.org.uk/; Grant No. NE/L002493/1 and by Loughborough University). GM was partly supported by the Swedish research Council Vetenskapsrdet (Grant. No. 2016-03724).

Conflict of interest

The authors declare that they have no conflict of interest.

References

[1] J. C. Gill and B. D. Malamud, "Reviewing and visualizing the interactions of natural hazards," *Reviews of Geophysics*, vol. 52, no. 4, pp. 680–722, 2014.

[2] J. Zscheischler, S. Westra, B. van den Hurk, S. Seneviratne, P. Ward, A. Pitman, A. AghaKouchak, D. Bresch, M. Leonard, T. Wahl, and X. Zhang, "Future climate risk from compound events," *Nature Climate Change*, vol. 8, no. 6, pp. 469–477, 2018.

[3] J. Zscheischler and S. I. Seneviratne, "Dependence of drivers affects risks associated with compound events," *Science advances*, vol. 3, no. 6, p. e1700263, 2017.

[4] M. Leonard, S. Westra, A. Phatak, M. Lambert, B. van den Hurk, K. McInnes, J. Risbey, S. Schuster, D. Jakob, and M. Stafford-Smith, "A compound event framework for understanding extreme impacts," *Wiley Interdisciplinary Reviews: Climate Change*, vol. 5, no. 1, pp. 113–128, 2014.

[5] UNDRR, "UN Sendai Framework for Disaster Risk Reduction (Terminology)," tech. rep., 2017.

[6] J. C. Gill and B. D. Malamud, "Hazard interactions and interaction networks (cascades) within multi-hazard methodologies," *Earth System Dynamics*, vol. 7, no. 3, pp. 659–679, 2016.

[7] J. C. Gill and B. D. Malamud, "Anthropogenic processes, natural hazards, and interactions in a multi-hazard framework," *Earth-Science Reviews*, vol. 166, pp. 246–269, 2017.

[8] M. S. Kappes, M. Keiler, K. von Elverfeldt, and T. Glade, "Challenges of analyzing multi-hazard risk: a review," *Natural Hazards*, vol. 64, no. 2, pp. 1925–1958, 2012.

[9] B. Liu, Y. L. Siu, and G. Mitchell, "Hazard interaction analysis for multi-hazard risk assessment: a systematic classification based on hazard-forming environment," *Natural Hazards and Earth System Sciences*, vol. 16, pp. 629–642, mar 2016.

[10] S. Terzi, S. Torresan, S. Schneiderbauer, A. Critto, M. Zebisch, and A. Marcomini, "Multi-risk assessment in mountain regions: A review of modelling approaches for climate change adaptation," *Journal of Environmental Management*, vol. 232, pp. 759–771, 2019.

[11] A. AghaKouchak, L. S. Huning, O. Mazdiyasni, I. Mallakpour, F. Chiang, M. Sadegh, F. Vahedifard, and H. Moftakhari, "How do natural hazards cascade to cause disasters?," *Nature*, vol. 561, no. 7724, pp. 458–460, 2018.

[12] L. Collet, S. Harrigan, C. Prudhomme, G. Formetta, and L. Beevers, "Future hot-spots for hydro-hazards in Great Britain: a probabilistic assessment," *Hydrology and Earth System Sciences*, vol. 22, no. 10, pp. 5387–5401, 2018.

[13] F. Vahedifard, A. AghaKouchak, and N. H. Jafari, "Compound hazards yield Louisiana flood," *Science*, vol. 353, pp. 1374 LP – 1374, sep 2016.

[14] S. Fuchs, M. Keiler, and A. Zischg, "A spatiotemporal multi-hazard exposure assessment based on property data," *Natural Hazards and Earth System Sciences*, vol. 15, no. 9, pp. 2127–2142, 2015.

[15] C. L. E. Franzke, "Impacts of a Changing Climate on Economic Damages and Insurance," *Economics of Disasters and Climate Change*, vol. 1, no. 1, pp. 95–110, 2017.

[16] P. De Luca, J. K. Hillier, R. L. Wilby, N. W. Quinn, and S. Harrigan, "Extreme multi-basin flooding linked with extra-tropical cyclones," *Environmental Research Letters*, vol. 12, no. 11, p. 114009, 2017.

[17] P. De Luca, C. Harpham, R. L. Wilby, J. K. Hillier, C. L. E. Franzke, and G. C. Leckebusch, "Past and projected weather pattern persistence with associated multi-hazards in the British Isles," *Under review https://eartharxiv.org/ghuzv/*, 2019.

[18] P. De Luca, G. Messori, R. L. Wilby, M. Mazzoleni, and G. Di Baldassarre, "Concurrent wet and dry hydrological extremes at the global scale," *Earth Syst. Dynam. Discuss.*, pp. 1–24, jun 2019.

[19] P. J. Ward, A. Couasnon, D. Eilander, I. D. Haigh, A. Hendry, S. Muis, T. I. E. Veldkamp, H. C. Winsemius, and T. Wahl, "Dependence between high sea-level and high river discharge increases flood hazard in global deltas and estuaries," *Environmental Research Letters*, vol. 13, no. 8, p. 84012, 2018.

[20] T. Ben-Ari, J. Boé, P. Ciais, R. Lecerf, M. Van der Velde, and D. Makowski, "Causes and implications of the unforeseen 2016 extreme yield loss in the breadbasket of France," *Nature Communications*, vol. 9, no. 1, p. 1627, 2018.

[21] E. Bevacqua, D. Maraun, I. Hobæk Haff, M. Widmann, and M. Vrac, "Multivariate statistical modelling of compound events via pair-copula constructions: analysis of floods in Ravenna (Italy)," *Hydrology and Earth System Sciences*, vol. 21, no. 6, pp. 2701–2723, 2017.

[22] M. I. Brunner, R. Furrer, and A.-c. Favre, "Modeling the spatial dependence of floods using the Fisher copula," no. April, pp. 1–25, 2018.

[23] D. Lee and H. Joe, "Multivariate extreme value copulas with factor and tree dependence structures," *Extremes*, vol. 21, no. 1, pp. 147–176, 2018.

[24] J. T. Shiau, "Fitting drought duration and severity with two-dimensional copulas," *Water Resources Management*, vol. 20, no. 5, pp. 795–815, 2006.

[25] M. Oesting and A. Stein, "Spatial modeling of drought events using max-stable processes," *Stochastic Environmental Research and Risk Assessment*, vol. 32, no. 1, pp. 63–81, 2018.

[26] Z. Wang, Y. Yan, X. Zhang, J. Yan, and X. Zhang, "Incorporating spatial dependence in regional frequency analysis," *Water Resources Research*, vol. 50, no. 12, pp. 9570–9585, 2014.

[27] C. Keef, J. Tawn, and C. Svensson, "Spatial risk assessment for extreme river flows," *Journal of the Royal Statistical Society. Series C: Applied Statistics*, vol. 58, no. 5, pp. 601–618, 2009.

[28] C. Keef, J. A. Tawn, and R. Lamb, "Estimating the probability of widespread flood events," *Environmetrics*, vol. 24, no. 1, pp. 13–21, 2013.

[29] J. Neal, C. Keef, P. Bates, K. Beven, and D. Leedal, "Probabilistic flood risk mapping including spatial dependence," *Hydrological Processes*, vol. 27, no. 9, pp. 1349–1363, 2013.

[30] L. J. Speight, J. W. Hall, and C. G. Kilsby, "A multi-scale framework for flood risk analysis at spatially distributed locations," *Journal of Flood Risk Management*, vol. 10, no. 1, pp. 124–137, 2017.

[31] F. Zheng, S. Westra, M. Leonard, and S. A. Sisson, "Modeling dependence between extreme rainfall and storm surge to estimate coastal flooding risk," *Water Resources Research*, vol. 50, no. 3, pp. 2050–2071, 2014.

[32] G. Kuczera, "Comprehensive atsite flood frequency analysis using Monte Carlo Bayesian inference," *Water Resources Research*, vol. 35, pp. 1551–1557, may 1999.

[33] H. H. Kwon, U. Lall, and S. J. Kim, "The unusual 20132015 drought in South Korea in the context of a multicentury precipitation record: Inferences from a nonstationary, multivariate, Bayesian copula model," *Geophysical Research Letters*, vol. 43, no. 16, pp. 8534–8544, 2016.

[34] S. Madadgar and H. Moradkhani, "Spatio-temporal drought forecasting within Bayesian networks," *Journal of Hydrology*, vol. 512, pp. 134–146, 2014.

[35] H. Yan and H. Moradkhani, "A regional Bayesian hierarchical model for flood frequency analysis," *Stochastic Environmental Research and Risk Assessment*, vol. 29, no. 3, pp. 1019–1036, 2014.

[36] T. Ghizzoni, G. Roth, and R. Rudari, "Multivariate skew-t approach to the design of accumulation risk scenarios for the flooding hazard," *Advances in Water Resources*, vol. 33, no. 10, pp. 1243–1255, 2010.

[37] T. Ghizzoni, G. Roth, and R. Rudari, "Multisite flooding hazard assessment in the Upper Mississippi River," *Journal of Hydrology*, vol. 412-413, pp. 101–113, 2012.

[38] Z. Hao, F. Hao, V. P. Singh, Y. Xia, C. Shi, and X. Zhang, "A multivariate approach for statistical assessments of compound extremes," *Journal of Hydrology*, vol. 565, pp. 87–94, 2018.

[39] M. G. Genton, S. A. Padoan, and H. Sang, "Multivariate max-stable spatial processes," *Biometrika*, vol. 102, pp. 215–230, feb 2015.

[40] O. Martius, S. Pfahl, and C. Chevalier, "A global quantification of compound precipitation and wind extremes," *Geophysical Research Letters*, vol. 43, pp. 7709–7717, jul 2016.

[41] D. Waliser and B. Guan, "Extreme winds and precipitation during landfall of atmospheric rivers," *Nature Geoscience*, vol. 10, p. 179, feb 2017.

[42] D. Faranda, G. Messori, and P. Yiou, "Dynamical proxies of North Atlantic predictability and extremes," *Scientific Reports*, vol. 7, p. 41278, 2017.

[43] G. Messori, R. Caballero, and D. Faranda, "A dynamical systems approach to studying midlatitude weather extremes," *Geophysical Research Letters*, vol. 44, pp. 3346–3354, apr 2017.

[44] V. Lucarini, D. Faranda, J. M. Freitas, M. Holland, T. Kuna, M. Nicol, and S. Vaienti, *Extremes and recurrence in dynamical systems*. John Wiley & Sons, 2016.

[45] J. G. Pinto, N. Bellenbaum, M. K. Karremann, and P. M. Della-Marta, "Serial clustering of extratropical cyclones over the North Atlantic and Europe under recent and future climate conditions," *Journal of Geophysical Research: Atmospheres*, vol. 118, pp. 12,412–476,485, nov 2013.

[46] G. J. van Oldenborgh, D. B. Stephenson, A. Sterl, R. Vautard, P. Yiou, S. S. Drijfhout, H. von Storch, and H. van den Dool, "Drivers of the 2013/14 winter floods in the UK," *Nature Climate Change*, vol. 5, p. 490, may 2015.

[47] C. Huntingford, T. Marsh, A. A. Scaife, E. J. Kendon, J. Hannaford, A. L. Kay, M. Lockwood, C. Prudhomme, N. S. Reynard, S. Parry, J. A. Lowe, J. A. Screen, H. C. Ward, M. Roberts, P. A. Stott, V. A. Bell, M. Bailey, A. Jenkins, T. Legg, F. E. L. Otto, N. Massey, N. Schaller, J. Slingo, and M. R. Allen, "Potential influences on the United Kingdom's floods of winter 2013/14," *Nature Climate Change*, vol. 4, no. 9, pp. 769–777, 2014.

[48] S. Wild, D. Befort, and G. C. Leckebusch, "Was the Extreme Storm Season in Winter 2013/14 Over the North Atlantic and the United Kingdom Triggered by Changes in the West Pacific Warm Pool?, [in Explaining Extremes of 2014 from a Climate Perspective]," *Bull. Amer. Meteor. Soc.*, vol. 96, no. 12, 2015.

[49] L. Trenary, T. DelSole, M. K. Tippett, and B. Doty, "Was the cold eastern US winter of 2014 due tro Increased Variability?, [in Explaining Extremes of 2014 from a Climate Perspective]," *Bull. Am. Meteorol. Soc*, vol. 96, no. 12, 2015.

[50] M.-Y. Lee, C.-C. Hong, and H.-H. Hsu, "Compounding effects of warm sea surface temperature and reduced sea ice on the extreme circulation over the extratropical North Pacific and North America during the 20132014 boreal winter," *Geophysical Research Letters*, vol. 42, pp. 1612–1618, mar 2015.

[51] G. Messori, R. Caballero, and M. Gaetani, "On cold spells in North America and storminess in western Europe," *Geophysical Research Letters*, vol. 43, pp. 6620–6628, jun 2016.

[52] D. P. Dee, S. M. Uppala, A. J. Simmons, P. Berrisford, P. Poli, S. Kobayashi, U. Andrae, M. A. Balmaseda, G. Balsamo, P. Bauer, P. Bechtold, A. C. M. Beljaars, L. van de Berg, J. Bidlot, N. Bormann, C. Delsol, R. Dragani, M. Fuentes, A. J. Geer, L. Haimberger, S. B. Healy, H. Hersbach, E. V. Hólm, L. Isaksen, P. Kållberg, M. Köhler, M. Matricardi, A. P. McNally, B. M. Monge-Sanz, J.-J. Morcrette, B.-K. Park, C. Peubey, P. de Rosnay, C. Tavolato, J.-N. Thépaut, and F. Vitart, "The ERA-Interim reanalysis: configuration and performance of the data assimilation system," *Quarterly Journal of the Royal Meteorological Society*, vol. 137, no. 656, pp. 553–597, 2011.

[53] A. G. Barnston and R. E. Livezey, "Classification, Seasonality and Persistence of Low-Frequency Atmospheric Circulation Patterns," 1987.

[54] D. Faranda, G. Messori, and P. Yiou, "Diagnosing concurrent drivers of weather extremes: application to hot and cold days in North America," *Under review*, 2019.

[55] D. Faranda, G. Messori, M. C. Alvarez-Castro, and P. Yiou, "Dynamical properties and extremes of Northern Hemisphere climate fields over the past 60 years," *Nonlin. Processes Geophys.*, vol. 24, pp. 713–725, dec 2017.

[56] D. Faranda, M. C. Alvarez-Castro, G. Messori, D. Rodrigues, and P. Yiou, "The hammam effect or how a warm ocean enhances large scale atmospheric predictability," *Nature Communications*, vol. 10, no. 1, p. 1316, 2019.

[57] A. Hochman, P. Alpert, T. Harpaz, H. Saaroni, and G. Messori, "A new dynamical systems perspective on atmospheric predictability: Eastern Mediterranean weather regimes as a case study," *Science Advances*, vol. 5, p. eaau0936, jun 2019.

[58] D. Rodrigues, M. C. Alvarez-Castro, G. Messori, P. Yiou, Y. Robin, and D. Faranda, "Dynamical Properties of the North Atlantic Atmospheric Circulation in the Past 150 Years in CMIP5 Models and the 20CRv2c Reanalysis," *Journal of Climate*, vol. 31, pp. 6097–6111, may 2018.

[59] D. Faranda, G. Messori, and S. Vannitsem, "Attractor dimension of time-averaged climate observables: insights from a low-order ocean-atmosphere model," *Tellus A: Dynamic Meteorology and Oceanography*, vol. 71, pp. 1–11, jan 2019.

[60] M. Süveges, "Likelihood estimation of the extremal index," *Extremes*, vol. 10, no. 1, pp. 41–55, 2007.

[61] M. Abadi, A. C. M. Freitas, and J. M. Freitas, "Dynamical counterexamples regarding the Extremal Index and the mean of the limiting cluster size distribution," *arXiv preprint arXiv:180802970*, 2018.

[62] A. H. Fink, T. Brücher, V. Ermert, A. Krüger, and J. G. Pinto, "The European storm Kyrill in January 2007: synoptic evolution, meteorological impacts and some considerations with respect to climate change," *Nat. Hazards Earth Syst. Sci.*, vol. 9, pp. 405–423, mar 2009.

[63] D. A. Lavers, R. P. Allan, E. F. Wood, G. Villarini, D. J. Brayshaw, and A. J. Wade, "Winter floods in Britain are connected to atmospheric rivers," *Geophysical Research Letters*, vol. 38, no. 23, pp. 1–8, 2011.

[64] T. Matthews, C. Murphy, R. L. Wilby, and S. Harrigan, "A cyclone climatology of the British-Irish Isles 18712012," *International Journal of Climatology*, vol. 36, pp. 1299–1312, mar 2016.

[65] A. B. Pieri, J. von Hardenberg, A. Parodi, and A. Provenzale, "Sensitivity of Precipitation Statistics to Resolution, Microphysics, and Convective Parameterization: A Case Study with the High-Resolution WRF Climate Model over Europe," *Journal of Hydrometeorology*, vol. 16, pp. 1857–1872, may 2015.

[66] B. Bisselink and A. J. Dolman, "Precipitation Recycling: Moisture Sources over Europe using ERA-40 Data," *Journal of Hydrometeorology*, vol. 9, pp. 1073–1083, oct 2008.

[67] S. Scher and G. Messori, "Predicting weather forecast uncertainty with machine learning," *Quarterly Journal of the Royal Meteorological Society*, vol. 144, pp. 2830–2841, oct 2018.

[68] D. Lee, P. Ward, and P. Block, "Attribution of Large-Scale Climate Patterns to Seasonal Peak-Flow and Prospects for Prediction Globally," *Water Resources Research*, vol. 54, pp. 916–938, jan 2018.

[69] G. G. Nobre, B. Jongman, J. Aerts, and P. J. Ward, "The role of climate variability in extreme floods in Europe," *Environmental Research Letters*, vol. 12, no. 8, p. 84012, 2017.

[70] K. E. Taylor, R. J. Stouffer, and G. A. Meehl, "An Overview of CMIP5 and the Experiment Design," *Bulletin of the American Meteorological Society*, vol. 93, pp. 485–498, oct 2011.

[71] V. Eyring, S. Bony, G. A. Meehl, C. A. Senior, B. Stevens, R. J. Stouffer, and K. E. Taylor, "Overview of the Coupled Model Intercomparison Project Phase 6 (CMIP6) experimental design and organization," *Geosci. Model Dev.*, vol. 9, pp. 1937–1958, may 2016.

[72] J. Cohen, J. A. Screen, J. C. Furtado, M. Barlow, D. Whittleston, D. Coumou, J. Francis, K. Dethloff, D. Entekhabi, J. Overland, and J. Jones, "Recent Arctic amplification and extreme mid-latitude weather," *Nature Geoscience*, vol. 7, p. 627, aug 2014.

[73] E. A. Barnes, "Revisiting the evidence linking Arctic amplification to extreme weather in midlatitudes," *Geophysical Research Letters*, vol. 40, pp. 4734–4739, aug 2013.

[74] D. Coumou, G. Di Capua, S. Vavrus, L. Wang, and S. Wang, "The influence of Arctic amplification on mid-latitude summer circulation," *Nature Communications*, vol. 9, no. 1, p. 2959, 2018.

[75] J. A. Screen and I. Simmonds, "Amplified mid-latitude planetary waves favour particular regional weather extremes," *Nature Climate Change*, vol. 4, p. 704, jun 2014.